

# Outflow Feedback Regulated Massive Star Formation in Parsec-Scale Cluster Forming Clumps

Peng Wang<sup>1</sup>, Zhi-Yun Li<sup>2</sup>, Tom Abel<sup>1</sup> and Fumitaka Nakamura<sup>3</sup>

## ABSTRACT

We investigate massive star formation in turbulent, magnetized, parsec-scale clumps of molecular clouds including protostellar outflow feedback using three dimensional numerical simulations of effective resolution  $2048^3$ . The calculations are carried out using a block structured adaptive mesh refinement code that solves the ideal MHD equations including self-gravity and implements accreting sink particles. We find that, in the absence of regulation by magnetic fields and outflow feedback, massive stars form readily in a turbulent, moderately condensed clump of  $\sim 1,600 M_{\odot}$  (containing  $\sim 10^2$  initial Jeans masses), along with a cluster of hundreds of lower mass stars. The massive stars are fed at high rates by (1) transient dense filaments produced by large-scale turbulent compression at early times, and (2) by the clump-wide global collapse resulting from turbulence decay at late times. In both cases, the bulk of the massive star’s mass is supplied from outside a 0.1 pc-sized “core” that surrounds the star. In our simulation, the massive star is clump-fed rather than core-fed. The need for large-scale feeding makes the massive star formation prone to regulation by outflow feedback, which directly opposes the feeding processes. The outflows reduce the mass accretion rates onto the massive stars by breaking up the dense filaments that feed the massive star formation at early times, and by collectively slowing down the global collapse that fuel the massive star formation at late times. The latter is aided by a moderate magnetic field of strength in the observed range (corresponding to a dimensionless clump mass-to-flux ratio  $\lambda \sim$  a few); the field allows the outflow momenta to be deposited more efficiently inside the clump. We conclude that the massive star formation in our simulated turbulent, magnetized, parsec-scale clump is outflow-regulated and clump-fed (ORCF for short). An important

---

<sup>1</sup>KIPAC, SLAC, and Physics Department, Stanford University, Menlo Park, CA 94025

<sup>2</sup>Astronomy Department, P.O. Box 400325, University of Virginia, Charlottesville, VA 22904; zl4h@virginia.edu

<sup>3</sup>Faculty of Education, Niigata University, 8050 Ikarashi-2, Niigata 950-2181, Japan; also visiting astronomer at Institute of Space and Astronautical Science, Japan Aerospace Exploration Agency, 3-1-1 Yoshinodai, Sagamihara, Kanagawa 229-8510, Japan

implication is that the formation of low-mass stars in a dense clump can affect the formation of massive stars in the same clump, through their outflow feedback on the clump dynamics. In a companion paper, we discuss the properties of the lower mass cluster members formed along with the massive stars, including their mass distribution and spatial clustering.

## 1. Introduction

The most important factor that determines whether a massive star can form or not is its mass accretion rate (Larson & Starrfield 1971; for recent reviews, see McKee & Ostriker 2007; Zinnecker & Yorke 2007). It follows from the fact that the outward radiative force on the accretion flow onto a forming massive star increases rapidly with the stellar mass. If the mass accretion rate is too low, there would be insufficient ram pressure to overcome the radiation pressure near the dust sublimation radius, and the infall would be choked. In the spherical model of Wolfire & Cassinelli (1987), the required minimum accretion rate ranges from  $\sim 10^{-4}$  to  $\sim 10^{-3} M_{\odot}/\text{yr}$  for stars in the mass range  $30 - 100 M_{\odot}$ , although the requirement can be relaxed somewhat if the accretion flow is flattened, by, e.g., magnetic support (Nakano 1989) or rotation (Jijina & Adams 1996). In addition to overcoming the radiation pressure, a high accretion rate can also greatly modify the internal structure and appearance of a growing massive star (e.g., Hosokawa & Omukai 2009). The associated high accretion luminosity may help heat up the region surrounding the protostar, perhaps suppressing the potential fragmentation that may adversely affect massive star formation at the early stages (Krumholz & McKee 2008).

A high mass accretion rate may not be difficult to achieve in principle, given that most, if not all, massive stars are thought to form in dense, massive, cluster-forming clumps (McKee & Ostriker 2007; Zinnecker & Yorke 2007). For example, a parsec-sized dense clump of  $10^3 M_{\odot}$  would have an average density of  $6.8 \times 10^{-20} \text{ g cm}^{-3}$ , corresponding to a global free fall time  $t_{\text{c,ff}} = 0.26 \text{ Myr}$ . The ratio of the clump mass and free-fall time yields a characteristic accretion rate  $\dot{M}_{\text{c,ff}} = 3.9 \times 10^{-3} M_{\odot}/\text{yr}$  (e.g., Cesaroni 2005) which, if channeled to a single object, would have a sufficiently large ram pressure to overcome the radiation pressure from even the most massive stars. In practice, the mass accretion rate onto any individual star will be reduced relative to the characteristic free-fall rate by several factors, such as the turbulence, magnetic fields, protostellar outflows, and radiative feedback. These factors are included in our simulations, except the last one.

Supersonic turbulence is observed ubiquitously in dense clumps of star cluster and massive star formation (e.g., Garay 2005). The turbulence is expected to reduce the mass

accretion rate onto any individual star relative to  $\dot{M}_{c,ff}$  in at least two ways. First, it resists the global collapse, thereby reducing the total amount of gas that collapses into stars per unit time. Second, it fragments the clump material into many centers of collapse, creating a cluster of stars each accreting at a fraction of the total rate. These effects of the turbulence are difficult to quantify analytically; numerical simulations are required (Mac Low & Klessen 2004). For example, using SPH simulation with sink particles, Bonnell, Bate & Vine (2003) found that a dense turbulent clump of  $10^3 M_\odot$  in mass and 0.5 pc in radius (corresponding to  $\dot{M}_{c,ff} = 5.4 \times 10^{-3} M_\odot/\text{yr}$ ) produced a cluster of about 400 stars. In their simulation, the most massive star (of  $27 M_\odot$ ) formed from an average accretion rate of order  $\sim 10^{-4} M_\odot/\text{yr}$ , much smaller than the global free-fall rate. In this paper, we will explore the effects of the turbulence on the stellar mass accretion further with a grid-based code, Enzo, including adaptive mesh refinement (AMR) and sink particles. The grid-based code also enables us to quantify, in addition, the effects of magnetic fields, which are generally difficult to treat in SPH (see, however, Price & Bate 2008).

There is ample observational evidence for magnetic fields in regions of massive star formation. In the nearest region of active massive star formation, OMC1, the well-ordered polarization vectors of submillimeter dust continuum leave little doubt that the (slightly pinched) magnetic field is dynamically important (e.g., Vaillancourt et al. 2008). A CN Zeeman measurement yields a line-of-sight field strength of 0.36 mG, corresponding to a magnetic energy density that is higher than the turbulent energy density and a mass-to-flux ratio (before geometric correction) that is 4.5 times higher than the critical value  $(2\pi G^{1/2})^{-1}$  (Falgarone et al. 2008). The mass-to-flux ratio is close to the median value inferred by Falgarone et al. for a sample of a dozen or so high-mass star forming regions where the CN Zeeman measurements are made. Their best estimate for the mean dimensionless mass-to-flux ratio (in units of the critical value) is  $\lambda \sim 2$  after geometric corrections, although it can be uncertain by a factor of 2 in either direction. A goal of our calculations is to determine how a magnetic field of this magnitude affects the stellar mass accretion rate, using an MHD version of the Enzo code (Wang & Abel 2009).

The third element that we consider in this paper are protostellar outflows, which are routinely observed around forming stars of both low and high masses (see the review by Richer et al. 2000). Their effects are expected to be particularly important in the dense clumps of active cluster formation, where many stars are formed close together in both space and time (Li & Nakamura 2006; Norman & Silk 1980). A case in point is the dense clump associated with the reflection nebula NGC 1333 in the Perseus molecular cloud, which is sculpted by dozens of outflows detectable in CO, optical forbidden lines and H<sub>2</sub> emission (Sandell & Knee 2001; Walawender et al. 2008; Maret et al. 2009). The outflows appear to inject enough momentum into the dense clump to replenish the turbulence dissipated in this

region (see, however, Maury et al. 2009 for a discussion of NGC 2264, where the current generation of active outflows appear incapable of supporting the cluster-forming clump). It is possible that a good fraction, perhaps the majority, of the cluster members are formed during the time when the clump turbulence is driven by protostellar outflows (Nakamura & Li 2007, Matzner 2007, Carroll et al. 2008, Swift & Welch 2008). We will improve on the previous outflow feedback simulations of Nakamura & Li (2007) by including sink particles, making the outflow injection more continuous, and dramatically increasing the numerical resolution. These improvements enable us to evaluate the effects of the outflows on the accretion rates onto individual stars, especially massive stars, which are the focus of this paper. We will describe the properties of the lower mass cluster members formed in our simulations, including their mass distribution and spatial clustering, in a companion paper. The effects of radiative feedback, ignored in our current calculations, are discussed in § 5.4.

The rest of the paper is organized as follows. In § 2, we describe the numerical method and simulation setup. These are followed by two result sections, focusing first on the global star formation history and clump dynamics (§ 3) and then on the massive stars (§ 4). We find that the massive stars in our simulations are formed through neither the collapse of pre-existing 0.1 pc-sized turbulent cores nor competitive accretion; their formation is controlled to a large extent by the clump dynamics, which are found to be regulated strongly by the collective outflow feedback from all accreting stars and, to a lesser extent, by a moderate magnetic field. In § 5, we discuss this new scenario of “outflow-regulated clump-fed” (ORCF for short) massive star formation and contrast it with the existing scenarios. The last section contains a brief summary.

## 2. Numerical Method and Simulation Setup

### 2.1. Magnetohydrodynamics

Our simulations are performed using the parallel AMR code, Enzo, with a newly added solver for unsplit conservative hydrodynamics and magnetohydrodynamics (Wang & Abel 2009). As usual, at the heart of the MHD solver lies the enforcement of the divergence-free condition  $\nabla \cdot B = 0$ . There are three classes of method for this purpose: constraint transport (CT, Evans & Hawley 1988), projection method and hyperbolic clean (see, e.g., Tóth 2000 for a review). We have evaluated all these methods and found that divergence cleaning is most suitable for the problem at hand, which involves rather extreme variation in physical quantities (including the field strength) due to both gravitational collapse and protostellar outflows. The fast and robust method of hyperbolic clean of Dedner et al. (2002) is adopted. It enables us to follow the formation of hundreds of stars over several dynamical times. We

monitor the value of  $\nabla \cdot B$  to ensure that it is small in all of our MHD simulations.

## 2.2. Sink Particles: Creation, Accretion and Merging

Truelove et al. (1997) pointed out that in order to avoid artificial fragmentation, one need to use at least four cells to resolve the Jeans length. For a given cell size at the finest level of refinement, the condition translates into a maximum density, which we will call the “Jeans density”, above which artificial fragmentation may happen. Since it is difficult in large-scale simulations such as ours to resolve the Jeans length all the way to the stellar density, sink particles are used to handle the gravitational collapse beyond the Jeans density. This approach has previously been successfully used in both SPH (e.g., Bate et al. 1995) and grid-based simulations of star formation (e.g., Krumholz et al. 2004; Offner et al. 2009).

Our procedure for implementing the sink particles is as follows. When a cell violates the Truelove criterion on the highest refinement level, a sink particle is inserted at the center of that cell. The initial mass of the sink particle is calculated such that after subtracting the sink mass, the cell will be at the Jeans density. The initial velocity of the sink particle is calculated using momentum conservation.

After creation, the sink particle accretes gas from its host cell according to a prescription inspired by the Bondi-Hoyle (BH) formula (Ruffert 1994),

$$\dot{M}_{BH} = 4\pi\rho_\infty r_{BH}^2 \sqrt{1.2544c_\infty^2 + v_\infty^2}, \quad (1)$$

where  $r_{BH}$  is the Bondi radius,  $\rho_\infty, v_\infty$  and  $c_\infty$  are the gas density, velocity and sound speed of the (uniform) medium far from the point mass.

Even though equation (1) is not strictly applicable to the highly turbulent medium under investigation, we will follow Krumholz et al. (2004) and use it as a guide to construct a prescription for sink particle accretion. Since the cloud material is assumed isothermal, it is natural to set  $c_\infty$  to the isothermal sound speed  $c_s$ . For  $v_\infty$ , we adopt the simple prescription  $v_\infty = v_{cell} - v_{sink}$ , where  $v_{cell}$  is the flow velocity in the cell and  $v_{sink}$  the velocity of the sink particle. We compute the Bondi radius in equation (1) using  $r_{BH} = GM_{sink}/(c_s^2 + v_\infty^2)$  where  $M_{sink}$  is the sink mass. If  $r_{BH}$  is smaller than the cell length  $\Delta x$ , the cell density  $\rho_{cell}$  is used for  $\rho_\infty$ . Otherwise an extrapolation assuming an  $r^{-1.5}$  density profile is used. In other words, we set  $\rho_\infty = \rho_{cell} \min[1.0, (\Delta x/r_{BH})^{1.5}]$ , where  $\Delta x = 200$  AU is the size of our finest cells. The amount of gas accreted during a single time step  $\Delta t$  is then  $\dot{M}_{BH}\Delta t$ . The amount may or may not match the true value exactly at any given time, given the crudeness of the above prescription. This deficiency is corrected in a second step, through sink particle merging.

Sink particle merging is needed not only to ensure the correctness of the mass accretion algorithm, but also to save computation time when many sink particles are created. It is a tricky problem, because we want to eliminate, on the one hand, the artificial particles created by the mismatch between the true accretion rate and that given by equation (1), and to preserve, on the other hand, the legitimate stellar seeds. It requires sub-grid information that is not available in the simulation. At this early stage in the development of the sink particle technique, our design principle of the merging recipe is to make it as simple as possible and with as few parameters as possible. We have experimented with a number of recipes, and settled on one with two parameters: a merging mass  $M_{merg}$  and a merging distance  $l_{merg}$ . Using  $M_{merg}$  we divide the sink particles into a “small” and a “big” group. At every time step, the merging is done in two steps. First, for each small particle, we search within the merging distance for its nearest big particle. If the search is successful, we merge this particle to the found big particle. Second, for all small particles that remain after the first step, we group them use a Friend-of-Friend algorithm with the merging distance  $l_{merg}$  as the linking length (Davis et al. 1985). In this work, we use  $M_{merg} = 0.01 M_{\odot}$  and  $l_{merg} = 5\Delta x$ , which is about 1000 AU. Experimentation shows that increasing  $M_{merg}$  to  $0.1 M_{\odot}$  or  $l_{merg}$  to  $10\Delta x$  does not change the star formation rate or the stellar mass distribution significantly. Lowering the merging distance to  $3\Delta x$  has little effect on the total star formation rate, but can change the mass of a star by up to 50%, probably because the flow pattern within a few cells of a sink particle is not well resolved. The flow so close to a forming star may be strongly affected by radiative heating (Offner et al. 2009; Bate 2009), which is not included in our simulations. For these reasons, we believe that the properties of circumstellar disks and binaries may not be reliably captured by our simulation; they are not discussed further in the paper.

With the inclusion of sink particle merging, the crude prescription for sink particle accretion based on the BH formula (1) does not appear to pose any serious problem. We have experimented with changing the parameters in the formula and did not see any significant difference in either the stellar mass accretion rate or the final stellar mass distribution. As stressed by Krumholz et al. (2004), the reason is probably that, when the BH formula underestimates the true accretion rate, the sink particle creation routine would transform the un-accreted gas into small sink particles, which would merge quickly with the original particle and restore the correct rate. On the other hand, when the BH formula overestimates the true rate, which happens rarely and only when the sink particle is massive, the accretion flow is typically supersonic near the particle, and the over-accretion does not affect the flow further away. To avoid numerical instabilities, we restrict the maximum amount of the gas accreted in a single time-step to be less than 25% of the cell mass.

Finally, the gravity of the sink particles is calculated using the standard particle-mesh

method, and their positions and velocities are updated using the leapfrog method.

### 2.3. Protostellar Outflows

Protostellar outflows are a crucial element of our model. In large-scale global simulations such as ours, it is unfortunately impossible to follow their production from first principles. An observationally motivated prescription is used instead. We assume that the protostellar outflow momentum injection rate is proportional to the stellar mass accretion rate, with a mass dependent proportionality constant  $P_* = P_0(M_*/M_0)^{1/2}$  where  $P_0 = 16$  km/s and  $M_0 = 1 M_\odot$ . The mass dependence is chosen to reflect the fact that the outflows from high mass stars tend to be more powerful even after correcting for their larger masses (Richer et al. 2000, D. Shepherd, private communication). We represent the outflow by injecting a momentum  $\Delta P = P_*\Delta M$  into the surrounding gas every time the sink particle has gained a mass increment  $\Delta M$ . Ideally, one would like to make  $\Delta M$  as small as possible, to render the injection continuous. However, we find continuous injection is too time consuming, because of the small Courant timestep associated with the fast outflow speed and small grid size near the sink particles. Furthermore, if  $\Delta M$  is much less than the mass of an injecting cell, the injected momentum would have little dynamical effect on the cell. These considerations led us to adopt  $\Delta M = 0.1 M_\odot$ . We have experimented with  $\Delta M = 0.2 M_\odot$ , and it did not change the results significantly. To avoid too high an outflow speed when a surrounding cell happens to have a low density, we take 10% $\Delta M$  out of the sink particle, and divide it evenly between the injecting cells. For simplicity, we inject the momentum in a bipolar jet, with the jet direction parallel (and anti-parallel) to the local magnetic field direction of the host cell when the jet is first injected (the jet direction is kept fixed in time) and a jet width of five finest cells.

### 2.4. Initial and Boundary Conditions

We consider a dense clump of molecular cloud that has an initial density profile with a uniform central region,

$$\rho(r) = \frac{\rho_c}{1 + (r/r_c)^2}, \quad (2)$$

where  $r_c = L/6$  and  $L$  is the length of the simulation box. The central density  $\rho_c = 1.0 \times 10^{-19}$  g cm<sup>-3</sup> and the box size is  $L = 2$  pc. This gives a cloud mass within a sphere of 1 pc in radius of  $M_s = 1215 M_\odot$ . Since a square box with  $L = 2$  pc is used, the total mass is somewhat larger, with  $M_{tot} = 1641 M_\odot$ . Our choice of cloud density, mass and mass distribution

is motivated by observations of infrared dark clouds (e.g., Butler & Tan 2009), which are thought to be future sites of cluster and massive star formation; they tend to be centrally condensed even before the onset of massive star formation.

The equation of state is isothermal, with a sound speed  $c_s = 0.265$  km/s, which corresponds to a temperature of  $T = 20$  K for a mean molecular weight  $\mu = 2.33$ .

A cloud with a density profile given by equation (2) has a gravitational potential energy  $E_G = 0.7GM_s^2/R$ , which yields a virial parameter  $\alpha_{vir} = 2E_K/E_G = R\sigma^2/(0.7GM_s)$ , where  $\sigma$  is the 3D rms velocity. In terms of the 3D Mach number  $\mathcal{M} \equiv \sigma/c_s$ , we have

$$\alpha_{vir} = 1.5 \left( \frac{\mathcal{M}}{9} \right). \quad (3)$$

The initial Mach number is set to  $\mathcal{M} = 9$ . Following the standard treatment in supersonic turbulence simulations (e.g. Mac Low et al. 1998), we impose a velocity field of power spectrum  $v_k^2 \propto k^{-4}$  with a minimum wave number 2 and maximum wave number 10 in units of inverse box length.

In models with a magnetic field, the field is assumed to be initially uniform in the  $z$  direction, with a strength given by

$$B_0 = 1.0 \times 10^{-4} \left( \frac{\lambda_{tot}}{1.4} \right)^{-1} \text{ Gauss}, \quad (4)$$

where  $\lambda_{tot} \equiv 2\pi G^{1/2} M_{tot}/(\pi B_0 L^2/4) = 1.4$  is the mass-to-flux ratio in units of the critical value. Because the adopted density profile is centrally condensed, the central part of the clump within  $r_c$  has a larger mass-to-flux ratio  $\lambda_c = 2.5\lambda_{tot} = 3.3$ . Thus the envelope is more magnetized than the central part. Our adopted degree of magnetization is in the range inferred by Falgarone et al. (2008).

For all simulations, the top grid has resolution  $128^3$  and the maximum refinement level is 4, which corresponds to a highest resolution of 200 AU. With this resolution and our sink particle algorithms, the risk of over producing low mass stars is reduced in our model even though we do not include radiative heating, which happens predominantly on the disk scales (Krumholz et al. 2007, Bate 2009). We will not be confident about the mass spectrum at the lowest mass end. However, the formation of massive stars, the main focus of this paper, is adequately resolved.

The boundary condition is periodic for all hydro and MHD quantities and gravity. In the model with protostellar outflows, to prevent the high speed outflows from re-entering the other side of the boundary and thus artificially increasing their effects, we reduce their speeds by a factor of 10 when they reach the boundary.



We consider four models of increasing complexities, starting with a base model (BASE) that is initially neither turbulent nor magnetized. We then add to this base model, one by one, an initial turbulence (HD), magnetic fields (MHD) and outflows (WIND). The models are summarized in Table 1 and discussed in turn below. Movies for the HD, MHD and WIND models are included in the electronic version of the paper.

### 3. Star Formation History and Global Gas Dynamics

Our centrally condensed clump described in § 2.4 contains many thermal Jeans masses. In the absence of any support in addition to thermal pressure, the clump collapses dynamically towards the center, forming an object within 0.2 Myr (see Fig. 1), close to the free-fall time of the central plateau part of the initial clump configuration  $t_{\text{ff},0} = 0.21$  Myr. There is a rapid initial increase in the mass accretion rate, characteristic of free-fall collapse of regions of flat density distribution. The accretion rate settles into a more or less constant value, as the material in the envelope part of the initial clump (that has an  $r^{-2}$  density distribution) starts to fall into the center. This nearly constant rate of mass accretion is reminiscent of the collapse of the singular isothermal sphere (SIS; Shu 1977), although the rate  $\dot{M} \sim 2.5 \times 10^{-3} M_{\odot}/\text{yr}$  is  $\sim 500$  times larger than the standard Shu’s value of  $4.3 \times 10^{-6} M_{\odot}/\text{yr}$  for 20 K gas. It is, however, close to the characteristic free-fall rate for the clump as a whole,  $\dot{M}_{\text{c,ff}} = 2.9 \times 10^{-3} M_{\odot}/\text{yr}$  (also plotted on Fig. 1 for comparison). The large characteristic accretion rate predisposes the clump to massive star formation, although this tendency can be weakened or even suppressed by various factors, including turbulence.

Turbulence reduces the total rate of mass accretion onto all stars as long as it provides a significant global support to the clump. It is therefore not surprising to find a smaller stellar mass accretion rate in the case with turbulence (Model HD) compared to the base model (BASE), especially at early times (see Fig. 1). The rate increases as the turbulence decays, reaching values of order  $2 \times 10^{-3} M_{\odot}/\text{yr}$ , not far below the characteristic free-fall rate  $\dot{M}_{\text{c,ff}}$ , at  $t \sim 0.5$  Myr, which is comparable to both the free-fall time at the average density of the clump and the crossing time for the initial turbulence. Thereafter, the clump dynamics is dominated by global collapse, as in the non-turbulent model BASE. The global collapse is illustrated in the first panel of Fig. 2, which plots the mass distribution and velocity field at the end of the simulation ( $t = 3 t_{\text{ff},0}$ ) on a slice through the most massive star. As expected, the dense materials are collected preferentially near the bottom of the gravitational potential well, where they are fed by the clump matter that falls towards the bottom.

The total star formation rate is lowered further by magnetic fields and outflows. Since the central plateau region of the clump has a mass-to-flux ratio that is significantly larger

than the critical value, the magnetic field there is not able to reduce the initial star formation rate significantly. However, the magnetic field becomes more important at late times, after the initial turbulence has decayed substantially and the more strongly magnetized clump envelope begins to collapse. The ensuing global collapse is retarded by the magnetic field in the cross-field direction. The retardation reduces the total stellar accretion rate by a moderate factor of 2-3.

The global collapse is even less prominent when outflows are included (the second panel of Fig. 2). The outflows have apparently supplied enough energy (and momentum) into the clump that the bulk of its material is prevented from either collapsing towards a global center or settling along field lines into a thin sheet (although some degree of flattening in the mass distribution is still evident). The feedback has kept the total mass accretion rate at only 10% of the characteristic free-fall rate (shown in Fig. 1 for comparison). The global support directly affects the properties of the massive stars that are formed in the clump, as we show next.

## 4. Massive Star Formation

In this section, we will concentrate on massive stars, defined somewhat arbitrarily as those sink particles with masses more than  $10 M_{\odot}$ . Our concentration on these stars is motivated by the fact that their formation mechanism is still under debate. We postpone a discussion of the properties of the lower mass stars to another publication.

### 4.1. Properties of Massive Stars

Massive stars are formed in all of the four simulations listed in Table 1. In the limit of no turbulence (Model BASE), all of the accreted mass goes to a single object at the center. At the end of the simulation ( $t = 2$ ), the object has grown to more than  $400 M_{\odot}$ , which is clearly unphysical. The addition of an initial turbulence in Model HD enabled the formation of eight massive sink particles by  $t = 3$ . The time evolution of the positions of these particles are shown in Fig. 3. There are two features worth noting. First, only five lines are clearly distinguishable in the plot. This is because the first 4 of the 8 stars are formed close together both in space and in time; they stay close together at all times, so that their trajectories are indistinguishable. For our main purpose of evaluating mass accretion rate, we will treat them as a single object. Second, the remaining four massive stars are formed at different times and locations. Two of them join the first object at later times to form a tight group,

while the other two merge into another system. We refer to the merged systems as group A and B respectively, and the massive stars formed at different times in each group as different generations. For example, A1 is the first generation of massive stars to form in group A. We will refer to all massive stars in each generation as “a massive object” (because they form at essentially the same time and same location, and partition of mass between the stars depends somewhat on the sink particle treatment). Some properties of the massive objects are listed in Tables 3-5 at three different times  $t = 3, 4$  and 5.525.

There are drastic differences between the massive objects formed in different simulations. At a relatively early time  $t = 3$  ( $\sim 0.6$  Myr, about one global free fall time; Table 2), 5 massive objects (8 massive stars) form in the HD Model, with a total mass of  $131 M_{\odot}$ , which is 37% of the stellar mass. The presence of a magnetic field in Model MHD reduces the number of massive objects (stars) to 3 (4), and their total mass to  $73.6 M_{\odot}$ , although the mass fraction of the massive stars remains similar (45%). When outflows are turned on (Model WIND), the formation of massive stars is suppressed up to this time, with no stars more massive than  $10 M_{\odot}$ .

Massive stars do form at later times in Model WIND. At  $t = 4$ , there are two massive stars ( $16.9$  and  $10.5 M_{\odot}$  each) formed, with a total mass of  $27.4 M_{\odot}$ , which is much less than the total mass of massive stars formed at the same time in Model MHD ( $183 M_{\odot}$ ). The difference re-enforces the notion that the outflows retard massive star formation. The massive stars do continue to grow with time, however. They attain  $46.4$  and  $16.7 M_{\odot}$  respectively near the end of the simulation at  $t = 5.5$  (about two global free fall times). They are each joined by another massive star, forming two loose groups. Together, the four massive stars contain  $86.9 M_{\odot}$ , accounting for 35% of all the stellar mass in the cluster.

## 4.2. Formation of the Most Massive Object

How do massive stars form in our simulations? To address this question, we will concentrate on the most massive object formed in each simulation, starting with the simpler, HD Model that has turbulence but neither magnetic fields nor outflow feedback.

### 4.2.1. Model HD

The most massive object, HD-A1 in Table 2, formally reached a mass of  $61.1 M_{\odot}$  at the end of the simulation ( $t = 3$  or  $0.63$  Myr). It is among the first objects to form, at a time  $t \sim 0.2$  Myr. The average mass accretion rate is therefore  $\dot{M}_{\text{ave}} \approx 1.5 \times 10^{-4} M_{\odot}/\text{yr}$ . The

instantaneous accretion rate for this object is shown in Fig. 4. It quickly rises to a plateau of  $\sim 10^{-4} M_{\odot}/\text{yr}$ , before jumping at  $t \sim 0.5$  Myr to a second plateau that is  $\sim 2.5$  higher. About equal amounts of mass ( $\sim 30 M_{\odot}$ ) are accreted in the two plateau phases. During the first plateau phase, the stellar mass increased by an order of magnitude, while the mass accretion rate stayed more or less constant. This behavior is characteristic of core collapse (such as the collapse of the singular isothermal sphere where the mass accretion rate is a constant, Shu 1977) rather than the Bondi-Hoyle type accretion which depends sensitively on the stellar mass. The rapid increase in mass accretion rate around  $\sim 0.5$  Myr is not triggered by any sudden increase in stellar mass, which again points to an external control of the mass accretion rate; it is caused by the onset of global collapse of the clump.

To examine the nature of the accreting flow before the global collapse in more detail, we plot in Fig. 5 the mass distribution, velocity field and gravitation potential at  $t = 1.5$ , when the eventual massive object A1 is still in an early stage of accretion. It is embedded in a dense filament, which is produced by converging flows in the turbulence (see also Banerjee, Pudritz & Anderson 2006). Here, the inclusion of self-gravity in the calculation is crucial. It allows the converged material to stay together, rather than re-bouncing and dispersing quickly; in other words, the self-gravity softens the high-speed collision that creates the filament.

The filament feeds the object at a high rate of  $\sim 10^{-4} M_{\odot}/\text{yr}$ , some 20 times the standard Shu’s rate for an singular isothermal sphere (SIS). As stressed by Banerjee et al. (2006), the high accretion rate is due to the rapid formation of non-equilibrium structures (dense filaments) that are fed continuously by converging flows (and are thus very different from the equilibrium SIS). Their existence does not depend on the stellar objects embedded in them; rather, the objects are produced by the runaway collapse of the densest parts of the filaments, often at the intersections with other filaments. In this sense, the formation of the most massive object in this early phase is not due to competitive accretion, since the gravity of the object is not the primary driver of the mass accumulation in the filaments; there are few objects to compete against at this stage of star formation in any case. It may be viewed as a special version of core collapse, in which the “core” is an over-dense, highly out-of-equilibrium filament that existed before the object and that continues to grow out of the converging flow even as part of it disappears into the collapsed object. The removal of dense gas from the filament via star formation also promotes further mass accumulation in the filament, by reducing its internal pressure and thus the resistance to further compression. In this picture, the massive star formation is simply part of the rapid “core” formation process. The use of sink particles in our simulation enables us to go beyond the calculations of Banerjee et al. (which stopped before significant mass accretion onto the stellar object) and follow the mass accretion for a long time, and to reveal a second phase of even more

rapid accretion, driven by global collapse.

The global collapse at the end of the pure hydro simulation ( $t=3$ ) was already shown in Fig. 2. It is further illustrated in Fig. 5, which shows the distribution of mass, velocity field and contours of gravitation potential in a sub-region centered on the most massive object, with the positions of stars superposed. It is clear that the global collapse has supplied the central region near the bottom of the gravitational potential well with plenty of dense material, which fuels both the enormous rate of total stellar mass accretion (close to the characteristic free-fall rate, see Fig. 1) and the high accretion rate of the most massive object, which is but one of many stars in the region. In this crowded region, competitive rather than core accretion is likely at work. The reason is that the stars in this region are not enveloped by permanent host cores, because the dense gas in the region is constantly drained onto stars and constantly replenished by the global collapse. The most massive object is located near the minimum of the global potential well and accretes the global collapse-fed material at a rate higher than any other object. Nevertheless, its accretion rate is only  $\sim 10\%$  of the total rate. In other words, the vast majority of the globally collapsing flow is diverted to stars other than the most massive object. Its accretion rate is large ( $\sim 2.5 \times 10^{-4} M_{\odot}/\text{yr}$ ) during this late phase only because of an even larger global collapse rate.

A common theme of the early and late phases of rapid accretion is that the dense gas that feeds the most massive object at a high rate is gathered by an agent external to the object. It is the converging flow set up by the initial turbulence in the early phase and the globally collapsing flow in the late phase. In this aspect, the formation mechanism is closer to core collapse than to competitive accretion. One may plausibly identify the dense filament in the early phase and the dense region at the bottom of the global gravitational potential well in the late phase as a McKee-Tan core (McKee & Tan 2003). However, the “cores” so identified are transient objects that are not in equilibrium. They are evolving constantly, with mass growing (from converging or collapsing flow) and depleting (into one or more collapsed objects) at the same time. The replenishment of dense gas in the “core” is the key to the long duration of high mass accretion rate for the most massive object, which is many times the free fall time of the small dense “core” and comparable to the global collapse time of the clump as a whole. In other words, there is no hint of any drop in the mass accretion rate after a finite reservoir of core material gets depleted over a (short) core free-fall time. Indeed, the nearly constant or increasing accretion rate for the most massive object highlights the important issue of when and how the mass accretion is terminated; there is an urgent need to tackle this issue if the final stellar mass is to be determined. We will return to a more detailed discussion of the nature of the massive star’s high accretion rate in the absence of magnetic fields and outflow feedback in § 5.1.

#### 4.2.2. Model MHD

The effect of the magnetic field in Model MHD on the mass accretion rate onto the most massive object is relatively modest (see Fig. 4). As in the HD case, there are two plateau phases. The first starts somewhat later than that in the HD case, indicating that the initiation of star formation in general and massive star formation in particular is somewhat delayed, as expected, because of magnetic cushion of turbulent compression. Once started, the accretion rate onto the most massive object is in fact slightly higher in the MHD case than in the HD case, indicating that the magnetic field does not significantly impede the initial phase of rapid mass accretion, which is enabled by the dense structures formed by turbulent compression. Indeed, dense structure formation is aided by a strong magnetic field, which forces the turbulent flows to collide along the field lines. When viewed in 3D, the dense structure resembles a warped, fragmented disk, with transient spirals that come and go. The spirals indicate significant levels of rotation on relatively small scales, which may hinder the stellar mass accretion due to centrifugal barriers.

The centrifugal barrier may be weakened or even removed by magnetic braking. Evidence for the braking is shown in Fig. 6, which shows a magnetic bubble driven from the central region, where active mass accretion is occurring. Magnetic braking driven bubbles provide a form of energy feedback that should accompany any star formed in a magnetized cloud (e.g., Draine 1980; Tomisaka 1998; Mellon & Li 2008; Hennebelle & Fromang 2008) but is absent from purely hydrodynamic models. We expect this form of feedback to become more important with a higher spatial resolution, since the rotating material closer to a star would be able to wrap the field lines more quickly (until the flux freezing under the ideal MHD assumption breaks down). Indeed, the protostellar outflow feedback may be viewed as a special form of this magnetic bubble-driven feedback, since the outflow is thought to be driven by the field lines that are forced to rotate rapidly by the circumstellar disks (Königl & Pudritz 2000; Shu et al. 2000).

Despite the feedback through the magnetic bubbles, large-scale collapse does occur at late times. When enough mass has been accumulated near the bottom of the gravitational potential well, the self-gravity of the accumulated gas overwhelms the magnetic tension forces, leading to a rapid cross-field collapse and an elevated, second phase of rapid mass accretion. The mass accretion is facilitated by the magnetic braking, which enables the high angular momentum material to sink closer to the center than it would be in the absence of the braking. The collapse is not as global as in the HD case, however, as shown in Fig. 7. At the end of the MHD simulation ( $t = 4$ ), the bulk of the clump material infalls towards the bottom of the potential well at a speed of order twice the sound speed or less, unlike in the HD case, where the infall is faster and more widespread. The collapse remains significantly

retarded by the magnetic tension except deep in the potential well.

#### 4.2.3. *Model WIND*

The combined effect of outflows and magnetic fields on the formation of the most massive object is much greater than that of magnetic fields alone. From Fig. 4, we find that, even though a massive star of more than  $45 M_{\odot}$  was eventually formed at the end of the WIND simulation, it took nearly  $10^6$  yrs to accrete the mass, with an average rate of only  $\sim 5 \times 10^{-5} M_{\odot}/\text{yr}$ . The accretion rate at early times is even lower, with a value of  $\sim 2 \times 10^{-5} M_{\odot}$  during the initial third of the time; it increases to  $\sim 4 \times 10^{-5} M_{\odot}/\text{yr}$  during the second third. These rates are about a factor of 5 lower than those in the HD and MHD models at comparable times. The question is: why does the most massive object accrete at such a low rate?

The basic reason is of course the outflows in the WIND model, which are much more powerful than the magnetic braking-driven bubbles that exist in the MHD case. The outflows modify both the mass distribution and velocity field, and thus the outcome of the gravitational dynamics. As a result, the most massive object forms at a somewhat different time and location. Despite the additional physics in both MHD and WIND models it is initially still embedded in a dense filament, as it is in the HD case. As discussed earlier, the filament is the key to the first, turbulence compression-induced phase of rapid mass accretion in the HD and MHD models. In the WIND model, accretion from the filament is reduced in two ways. First, there are several stars formed in the filament. They all emit outflows which tend to break the filament into smaller segments. Second, the outflows emerge more easily perpendicular to (rather than along) the filament. Once they break out, they blow against the converging flow and slow down the mass accumulation that feeds the growth of the filament in the first place.

As the outflows propagate to large distances, a fraction of their momentum is lost through the computation boundary. The remaining fraction is deposited in the lower density region that surrounds the denser region of active star formation near the bottom of the potential well. The momentum deposition allows the bulk of the clump material to be supported against rapid global collapse. The absence of a global collapse is illustrated in Fig. 8, which shows a rather chaotic velocity field that involves both infall and outflow. It is further quantified in Fig. 7, which shows that the mass-weighted infall speed toward the most massive object is subsonic over most of the volume, except within a radius of about 0.2 pc, where the speed becomes two to three times the sound speed (still much lower than the local free-fall speed). The slower infall leads to a smaller amount of dense gas accumulating

near the bottom of the potential well. The accumulated dense gas is also more fragmented because of interaction with outflows. Both factors limit the mass accretion rate onto the most massive object, especially at late times.

As in the HD and MHD cases, the most massive object is not formed out of a pre-existing dense core. The case against the pre-existing dense core picture is stronger in the WIND case, because it takes longer (nearly two global free-fall times) to accumulate the final mass, whereas a pre-existing dense core should collapse and exhaust its mass in a local (core) free-fall time, which should be a very small fraction of the global free-fall time. The slow accretion rate and long accretion time are clear evidence that the formation of the most massive object is controlled by the global clump dynamics in our WIND simulation.

## 5. Discussion

### 5.1. Unregulated Clump-Fed Massive Star Formation

Massive stars form quickly in our simulated parsec-scale clump in the absence of any magnetic field or outflow feedback (see Model HD). They are fueled by high mass accretion rates from either the dense filaments that are formed by turbulent compression or the clump-wide collapse due to the global turbulence dissipation. In both cases, the dense material that is depleted onto the massive star is constantly replenished. The replenishment is illustrated in the left panel of Fig. 9, where the mass of the most massive object is plotted as a function of time, along with the mass of the gas within a “core” of 0.1 pc in diameter around the object; the size was chosen to coincide with the fiducial value that McKee & Tan (2003) used to define their “turbulent cores.” It is clear that the “core” so defined has an initial mass that is well below the final mass of the most massive object, and thus cannot supply all of the mass of the object. As the object gains mass, the mass of the “core” stays roughly constant or even increases (rather than decreases), which demands that the core mass be replenished or fed from the surrounding clump. We are thus motivated to term this model the “clump-fed massive star formation” model.

Our “clump-fed massive star formation” model (CF model for short) contains elements of the two widely discussed scenarios for massive star formation in the literature: the turbulent core model of McKee & Tan (2003) and competitive accretion model of Bonnell et al. (2003). It has in common with the turbulent core model in that the mass accretion rate onto the massive star is not primarily determined by the star itself, but rather by the properties of the pre-existing gas that produces the seed of the star in the first place and that continues to feed the stellar growth; in other words, if the massive star were to be removed prematurely,



another seed would be produced in its place and grow to a high mass. It is the properties of the fueling gas that determine the stellar mass accretion rate and thus the stellar mass. McKee & Tan envisioned this gas to be a pre-existing massive turbulent core. It collapses to form the massive star, with a mass accretion rate that depends on the core structure. For example, if the turbulent core has a density profile of  $r^{-1.5}$ , the mass accretion rate would increase linearly with time  $t$  (McKee & Tan 2003). In our CF model, the pre-existing gas is the cluster-forming clump, which produces the transient dense material that feeds the massive star at a high rate through two mechanisms: (1) the collapse of the dense filaments produced by turbulent compression, as already emphasized by Banerjee et al. (2006), and (2) global collapse, driven by the turbulence decay in our simulations, but can in principle be caused by an external compression as well. The first mechanism depends on the detailed properties of the initial turbulence in the clump, which are not well constrained observationally. The second mechanism depends on the dissipation of (supersonic) turbulence that is inevitable, and should be more robust.

Our unregulated CF model has in common with the competitive accretion model in that a massive star can form even in the absence of a pre-existing turbulence-supported massive core and that the global gravitational potential and dynamics of the clump play an important, even the dominant, role in massive star formation. The latter is especially true at late times, when the global collapse feeds mass at a high rate to the compact region near the bottom of the potential well, where a large number of stars (including massive stars) are already present. In the absence of stellar feedback, competition for this clump-fed material in the crowded region is unavoidable. The most massive object tends to grow the fastest, mainly because it typically locates closest to the center of the potential, as emphasized by Bonnell et al. (2007). Although the numerical results of our grid-based AMR hydro simulations are in broad agreement with those of SPH simulations of Bonnell et al. (2003), we differ from their interpretation of the results regarding the formed stars, particularly as it relates to massive star formation. When a massive star is formed, the vast majority of the clump mass remains in the gas. The high accretion rates of the massive stars at late times of our hydro simulation derive directly from the global gas collapse. Even if there were no stars near the center of the collapse (or more likely the mass accretions onto individual stars are terminated by the stellar feedback), (other) massive stars can still form from scratch, as long as the collapse delivers mass to the center at a high enough rate. So we argue it is predominantly the structure and dynamics of the gaseous component that set the relevant physics in forming the massive stars rather than the properties of the stars made previously.

A moderately strong magnetic field (corresponding to the observationally inferred dimensionless mass-to-flux ratio of a few) does not qualitatively change the clump-fed picture for massive star formation by itself. As discussed in § 4.2.2, the magnetic field has relatively

little effect on the high mass accretion rate onto the most massive object induced by the initial turbulent compression and filament formation. Indeed, it is conducive to filament formation by guiding the converging flows to collide along the field lines. The magnetic field does slow down the global collapse-induced rapid accretion by a modest factor of a few. The basic ingredients of the CF model remain, however, as can be seen from the middle panel of Fig. 9. Specifically, the initial core mass is still much less the final mass of the most massive object, and most of the mass that goes into the object still needs to be replenished or fed from the surrounding clump. We conclude that the feeding processes for massive star formation are only weakly regulated by the magnetic field, perhaps because the field is only moderately strong (i.e., the clump is moderately supercritical), and it resists the feeding passively rather than actively (unlike the outflows, see below). The magnetic field does change the dynamical coupling between different parts of the clump, an important aspect of cluster and massive star formation that we plan to return to in a future investigation.

## 5.2. Outflow-Regulated Clump-Fed Massive Star Formation

Massive star formation through rapid accretion of the mass that is fed from outside the small region surrounding the forming star is particularly vulnerable to outflow feedback. This is because the feeding is directly opposed by the feedback. In the case of the rapid accretion fed by turbulent compression and filament formation, the filament is quickly chopped up into small segments by the outflows driven by the stars formed in it (see the outflow movie in the electronic version of the paper). The outflows also slow down any further mass accumulation in the filament after star formation is initiated. As a result, this mode of turbulent compression-fed massive star formation is strongly regulated, perhaps even choked off completely, by outflow feedback.

In the case of the rapid accretion fed by global collapse, the infall is countered by the outflows on all scales, especially on the global clump scale. The additional global support provided by the outflow feedback can reduce the total star formation rate by a large factor. This reduction affects the formation of all cluster members, especially the massive stars. This is because the massive stars receive a larger fraction of the collapse-fed material, and are thus more sensitive to the change of global clump dynamics. They also tend to complete their formation toward the end of cluster formation (even though their seeds tend to be among the first objects to form), making them more prone to the accumulative influence of multiple generations of outflows that precede their eventual formation. Since the outflows are believed to be driven by the release of gravitational binding energy from mass accretion in one form or another (Konigl & Pudritz 2000; Shu et al. 2000), and most of the accreted

mass goes to low-mass (rather than high-mass) stars for a Salpeter-like IMF, a large fraction if not the bulk of the outflow feedback should come from the low-mass stars. In this sense, the formation of low-mass stars in a dense clump can profoundly influence the formation of massive stars in the same clump, through their feedback on the clump dynamics. Whether massive stars eventually form or not in a dense clump depends on the extent to which all the outflows in the clump collectively regulate the global collapse and slow down the star formation. If the total star formation rate is reduced, for example, below the fiducial minimum rate for massive star formation,  $10^{-4}M_{\odot}/\text{yr}$ , no massive stars would form at all. In the opposite extreme where the outflows are weak and the feedback is not strong enough to reverse the global collapse, stars (especially massive stars) would form quickly, as in our pure hydro simulation.

The degree of outflow regulation will depend on the properties of the outflows, including their strengths and degrees of collimation, both of which are somewhat uncertain. What we have demonstrated explicitly through numerical simulation is that for well-collimated jets of reasonable strength the outflow feedback can prevent rapid global collapse, and keep the total star formation rate an order of magnitude below the characteristic free-fall rate. Massive stars do eventually form in our simulation that includes outflow feedback. It demonstrates that outflows can strongly regulate massive star formation, but do not necessarily quench it completely, especially in dense massive clumps with a high characteristic free-fall rate  $\dot{M}_{c,ff}$ . For such clumps, even when the bulk of the clump material is supported, a small fraction can still percolate down the global gravitational potential well, feeding the formation of massive stars near the center at a high enough rate.

The fact that our outflow-regulated massive star formation remains clump-fed rather than core-fed is illustrated in the right panel of Fig. 9. As in the HD and MHD models that do not have outflow feedback, the mass of the 0.1 pc-sized “core” that surrounds the most massive object in the WIND model is initially smaller than the final mass of the object, and does not decrease monotonically as the object accretes. Again, the bulk of the accreted stellar material must come from outside the “core,” which is an essential feature of our new scenario of outflow-regulated clump-fed (ORCF) massive star formation. In this picture, the parsec-scale cluster-forming clump, rather than a 0.1 pc-sized turbulent core, is the basic unit for massive star formation. As pointed out by Bonnell et al. (2007), a potential drawback of the turbulent core model is that massive, turbulence-supported, cores tend to fragment into many stars rather than collapse monolithically, although radiative feedback from the rapidly accreting massive stars can reduce the level of fragmentation (Krumholz & McKee 2008). Fragmentation is expected to be less of a problem in our clump-fed picture of massive star formation, since the material near the forming massive stars does not have to be supported by a strong turbulence; it is typically in a state of rapid collapse that feeds the growing

massive stars at a high rate, even though the clump as a whole may remain supported by (possibly outflow-driven) turbulence and, perhaps to a lesser extent, magnetic fields. If the parsec-scale dense clumps are indeed the basic units of massive star formation, how they form in the first place becomes an important problem that deserves close theoretical and observational attention.

### 5.3. A Condition for Massive Star Formation in Galaxy Formation Simulations

Massive stars play a dominant role in galaxy formation and evolution. Our ORCF scenario suggests a rough criterion for their formation that can be used in global galaxy formation simulations that reach the scale of the cluster forming clumps but do not resolve their internal structure.

The criterion is based on a threshold for mass accretion rate. A high mass accretion rate is needed not only to overcome the radiation pressure (Wolfire and Cassinelli 1987) and quench the development of HII region (Walmsley 1995), but also to satisfy observational constraints on the time scale of massive star formation. Wood & Churchwell estimated an age of  $\sim 10^5$  years for UC HII regions, which probably represent a relatively late stage of massive star formation, when the bulk of mass accretion has completed and the mass accretion rate becomes too low to trap the HII region (Churchwell 2002). The majority of the stellar mass may be accreted during the hot core (and perhaps hypercompact HII) phase, which lasts for a time of order  $10^5$  years or less (Kurtz et al. 2000). The relatively short time scale is also consistent with the dynamical times estimated for massive molecular outflows (which are presumably driven by rapid mass accretion during the main accretion phase, as in the case of low mass stars; e.g., Bontemps et al. 1996), which are typically of order  $10^5$  years or less (e.g., Zhang et al. 2005). If the time scale for massive star formation is indeed  $\sim 10^5$  yrs or less, to form a star of  $10M_{\odot}$ , a stellar mass accretion rate of  $\dot{M}_{\text{cr}} \sim 10^{-4} M_{\odot}/\text{yr}$  or more would be needed. A minimum requirement for massive star formation in a clump is that the characteristic free-fall rate  $\dot{M}_{\text{c,ff}}$  of the clump be greater than  $\dot{M}_{\text{cr}}$ .

The actual requirement will be more stringent. The accretion rate onto massive stars  $\dot{M}_{m^*}$  is related to the characteristic free-fall rate  $\dot{M}_{\text{c,ff}}$  of the dense clump by two factors:  $\dot{M}_{m^*} = \dot{M}_{\text{c,ff}} f_* f_{m^*}$ , where  $f_*$  is the actual rate of star formation normalized to the characteristic rate  $\dot{M}_{\text{c,ff}}$ , and  $f_{m^*}$  the fraction of the stellar mass accretion onto massive stars. We estimate the characteristic free-fall rate using the clump mass divided by the free-fall time at the average density

$$\dot{M}_{\text{c,ff}} \sim (8G/\pi^2)^{1/2}(M/R)^{3/2} \sim 1.9 \times 10^{-3}(M_3/R_{pc})^{3/2} M_{\odot}\text{yr}^{-1} \quad (5)$$

(where  $M_3$  is the clump mass in units of  $10^3 M_\odot$  and  $R_{pc}$  the clump radius in units of parsec), which yields  $2.5 \times 10^{-3} M_\odot/\text{yr}$  for a  $1200 M_\odot$  clump of 1 pc in radius, consistent with the value obtained in our reference model of non-turbulent collapse. The most uncertain factor in the above equation is perhaps  $f_*$ , the star formation rate compared to the characteristic free-fall rate. It depends on the extent to which the clump is supported globally. Decaying turbulence can provide significant global support within a turbulence decay time, when  $f_*$  can be significantly below unity. Unless the star formation is terminated in one decay time,  $f_*$  will eventually increase to a value not far from unity, as demonstrated in our HD model. A moderate magnetic field does not change the global support fundamentally, reducing  $f_*$  by a factor of only a few (see Model MHD). Together with the magnetic field, protostellar outflows can reduce  $f_*$  by an order of magnitude, to values of order  $\sim 0.1$ . The value of  $f_*$  may range from about 0.1 (before the virial turbulence decays away or after it is replenished) to close to unity (after the turbulence has decayed in the absence of magnetic support and turbulence replenishment). Krumholz & Tan (2007) argued that the star formation efficiency per free fall time is of order 10% or less, implying  $f_* \leq 0.1$ . Nakamura & Li (2007) found a similarly low value for the well-studied nearby clump of active cluster formation NGC 1333. Based on these results, we choose  $f_* \sim 0.1$  as the fiducial value. A smaller  $f_*$  would make it more difficult to form massive stars.

The value for the remaining factor  $f_{m*}$  can be constrained both observationally and numerically. If the Salpeter slope is universal for the upper part of the IMF, then about 1/3 of the stellar mass must reside in stars more massive than  $10 M_\odot$  (assuming a lower cut-off at  $0.3 M_\odot$ ). In this case,  $f_{m*} \sim 1/3$ , which is similar to the ratios obtained in our simulations, according to Tables 2-4. To be conservative, we assume that all of the massive star accretion rate,  $\dot{M}_{c,ff} f_* f_{m*}$ , goes to a single star. If more than one massive star are fed at this rate, the requirement for massive star formation would be more stringent.

Taken together, the above considerations yield the following mass accretion rate for a massive star:

$$\dot{M}_{m*} \sim 6.4 \times 10^{-5} M_\odot/\text{yr} \left( \frac{f_*}{0.1} \right) \left( \frac{f_{m*}}{1/3} \right) \left( \frac{M_3}{R_{pc}} \right)^{3/2}, \quad (6)$$

which has to exceed  $10^{-4} \dot{M}_{cr,-4} M_\odot/\text{yr}$  for massive star formation to actually occur ( $\dot{M}_{cr,-4}$  is the critical mass accretion rate for massive star formation in units of  $10^{-4} M_\odot/\text{yr}$ ). This yields a rough condition on the ratio of the mass and radius of the clump for massive star formation:

$$\frac{M_3}{R_{pc}} \gtrsim 1.4 \left( \frac{0.1}{f_*} \right)^{2/3} \left( \frac{1/3}{f_{m*}} \right)^{2/3} \dot{M}_{cr,-4}^{2/3}. \quad (7)$$

The significance of the above condition is that, if the fraction of the total stellar mass

going into massive stars ( $f_{m*}$ ) is constrained by observations, then whether a dense clump of a given mass and size (and thus given  $\dot{M}_{c,ff}$ ) can form massive stars or not boils down to the total star formation rate,  $f_*\dot{M}_{c,ff}$ . It depends on the clump dynamics, which is sensitive to the outflow feedback. The above condition is consistent with, for example, the sample of massive star forming clumps associated with water masers of Plume et al. (1997), which has a mean virial mass  $M_3 = 3.8$  and mean radius  $R_{pc} = 0.5$ . Their ratio of 7.6 is comfortably above the fiducial value of 1.4 in equation (7), indicating that massive stars can form, even when the total rate of star formation is an order of magnitude below the characteristic free-fall rate. A small value for the product  $f_*f_{m*}$  ( $\sim 1/30$ ) may be the reason for the massive star formation to occur predominantly in those special regions of molecular clouds—the massive dense clumps—that are both massive and compact.

#### 5.4. Limitations and Future Directions

The most severe limitation of the current work is perhaps the neglect of radiative feedback. Radiative heating changes the clump fragmentation behavior, especially close to the forming stars (Krumholz et al. 2007; Bate 2009). This effect was mimicked to some extent by the relatively large sink particle merging distance adopted in our simulations (with a length of 5 cells or  $10^3$  AU), which suppresses fragmentation on the small (mostly disk) scale. Furthermore, if our ORCF scenario is correct, the formation of massive stars may be more sensitive to the global clump dynamics (which are less affected by the radiative heating) than the gas properties close to the stars. Nevertheless, we believe that the formation of massive stars will benefit from the suppression of fragmentation by radiative heating, especially near the bottom of the gravitational potential well of the clump, where the thermal Jeans mass is formally smaller than the typical stellar mass. On small scales, radiative pressure may slow down the mass accretion onto individual massive stars somewhat, although the accretion may be enhanced to some extent by non-ideal MHD effects, such as ambipolar diffusion, which are not included in our ideal MHD calculations.

Another effect that we neglected was the HII region driven by the massive star’s UV radiation. The expansion of HII regions provides a way to remove the clump gas, and perhaps terminate the cluster formation. It needs to be included in future simulations that aim to model the entire history of cluster formation. Such studies may also need to include massive star winds, which are observed to have dramatic effects in some regions (e.g. the Carina Nebula, see Smith & Brooks 2008 for a review). They are the main alternative to the HII regions as the means for terminating the cluster formation.

A further limitation is the periodic boundary condition used in our simulation. It

precludes any communication between the cluster-forming clump and its surrounding environment. If there is energy injection into the dense clump from the ambient medium, the externally supplied energy may aid the outflows in regulating the cluster and massive star formation. Large-scale external compression may, on the other hand, lead to rapid clump collapse and massive star formation. In this case, the feeding of massive stars may extend beyond the parsec-scale clump, and the massive star formation may simply be part of the rapid clump formation.

## 6. Summary and Conclusion

We have carried out AMR-MHD simulations of massive star formation in dense, turbulent, parsec-scale clumps of cluster star formation including sink particles and outflow feedback. We find that, without regulation by magnetic fields and outflows, massive stars form quickly. They are fed at a high rate first by the converging flows in the initial turbulence and later by the global collapse induced by turbulence decay. A moderate magnetic field alone does not affect these feeding processes much. They are greatly modified, however, by a combination of protostellar outflows and magnetic fields. The outflows break up the turbulent compression-produced dense filaments that feed the massive stars at early times and stall the global collapse that fuel the massive star formation at later times. The outflow feedback is enhanced by a magnetic field, which links different parts of the clump together; the coupling makes the deposition of the outflow momenta in the clump more efficient. The magnetically-aided outflow feedback can in principle reduce the total rate of star formation below the critical mass accretion rate for massive star formation and suppress the massive star formation completely. In practice, whether massive stars form in a dense clump or not depends on the properties of the clump (particularly its mass and size) and the degree of magneto-outflow regulation of its star formation (see equation [7]). For parsec-scale clumps of order  $10^3 M_\odot$ , we have demonstrated explicitly through numerical simulations that the formation of massive stars is clump-fed and outflow-regulated. Additional simulations and analysis are needed to determine whether this new scenario of outflow-regulated clump-fed massive star formation is applicable to more massive and/or more compact dense clumps. In a companion paper, we will explore the effects of the outflow feedback on the lower mass cluster members.

ZYL is supported in part by NASA (NNG05GJ49G) and NSF (AST-030768) grants, and FN by a Grant-in-Aid for Scientific Research of Japan (20540228).

## REFERENCES

- Banerjee, R., Pudritz, R. E., & Anderson, D. W. 2006, *MNRAS*, 373, 1091
- Bate, M. R. 2009, *MNRAS*, 392, 1363
- Bate, M. R., & Bonnell, I. A. 2005, *MNRAS*, 356, 1201
- Bate, M. R., Bonnell, I. A., & Price, N. M. 1995, *MNRAS*, 277, 362
- Bonnell, I. A., Vine, S. G., & Bate, M. R. 2004, *MNRAS*, 349, 735
- Bonnell, I. A., Larson, R. B., & Zinnecker, H. 2007, *Protostars and Planets V*, 149
- Bontemps, S., Andre, P., Terebey, S., & Cabrit, S. 1996, *A&A*, 311, 858
- Butler, M. J., & Tan, J. C., 2009, *ApJ*, in press
- Carroll, J. J., Frank, A., Blackman, E. G., Cunningham, A. J., & Quillen, A. C. 2008, arXiv:0805.4645
- Cesaroni, R. 2005, in *Massive star birth: A crossroads of Astrophysics*, IAU Symposium 227, edited by Cesaroni, R.; Felli, M.; Churchwell, E.; Walmsley, M. (Cambridge: Cambridge University Press), p.59
- Churchwell, E. 2002, *ARA&A*, 40, 27
- Davis, M., Efstathiou, G., Frenk, C. S., & White, S. D. M. 1985, *ApJ*, 292, 371
- Dedner, A., Kemm, F., Krüner, D., Munz, C. -D., Schnitzer, T., & Wesenberg, M., 2002, *J. Comput. Phys.*, 175, 645
- Draine, B. T. 1980, *ApJ*, 241, 1021
- Evans, C. R., & Hawley, J. F. 1988, *ApJ*, 332, 659
- Falgarone, E., Troland, T. H., Crutcher, R. M., & Paubert, G. 2008, *A&A*, 487, 247
- Garay, G. 2005, *Massive Star Birth: A Crossroads of Astrophysics*, IAU Symposium 227, edited by Cesaroni, R.; Felli, M.; Churchwell, E.; Walmsley, M. (Cambridge: Cambridge University Press), p.86
- Hennebelle, P., & Fromang, S. 2008, *A&A*, 477, 9
- Hosokawa, T., & Omukai, K. 2009, *ApJ*, 691, 823



- Jijina, J., & Adams, F. C. 1996, *ApJ*, 462, 874
- Konigl, A., & Pudritz, R. E. 2000, *Protostars and Planets IV*, 759
- Krumholz, M. R., McKee, C. F., & Klein, R. I. 2004, *ApJ*, 611, 399
- Krumholz, M. R., Klein, R. I., & McKee, C. F. 2007, *ApJ*, 656, 959
- Krumholz, M. R., & McKee, C. F. 2008, *Nature*, 451, 1082
- Krumholz, M. R., & Tan, J. C. 2007, *ApJ*, 654, 304
- Kurtz, S., Cesaroni, R., Churchwell, E., Hofner, P., & Walmsley, C. M. 2000, *Protostars and Planets IV*, 299
- Larson, R. B., & Starrfield, S. 1971, *A&A*, 13, 190
- Li, Z.-Y., & Nakamura, F. 2006, *ApJ*, 640, L187
- Mac Low, M.-M., Klessen, R. S., Burkert, A., & Smith, M. D. 1998, *Physical Review Letters*, 80, 2754
- Mac Low, M.-M., & Klessen, R. S. 2004, *Reviews of Modern Physics*, 76, 125
- Maret, S., et al. 2009, arXiv:0904.0603
- Matzner, C. D. 2007, *ApJ*, 659, 1394
- Maury, A. J., Andre, Ph. & Li, Z.-Y. 2009, *AA*, 499, 175
- McKee, C. F., & Ostriker, E. C. 2007, *ARA&A*, 45, 565
- McKee, C. F., & Tan, J. C. 2003, *ApJ*, 585, 850
- Mellon, R. R., & Li, Z.-Y. 2008, *ApJ*, 681, 1356
- Nakamura, F., & Li, Z.-Y. 2007, *ApJ*, 662, 395
- Nakano, T. 1989, *ApJ*, 345, 464
- Norman, C., & Silk, J. 1980, *ApJ*, 238, 158
- Offner, S. R., Klein, R. I, McKee, C. F. & Krumholz, M. R. 2009, *ApJ*, submitted (arXiv:0904.2004v1)

- Plume, R., Jaffe, D. T., Evans, N. J., II, Martin-Pintado, J., & Gomez-Gonzalez, J. 1997, *ApJ*, 476, 730
- Price, D. J., & Bate, M. R. 2008, *MNRAS*, 385, 1820
- Richer, J. S., Shepherd, D. S., Cabrit, S., Bachiller, R., & Churchwell, E. 2000, *Protostars and Planets IV*, 867
- Ruffert, M., 1994, *ApJ*, 427, 342
- Sandell, G., & Knee, L. B. G. 2001, *ApJ*, 546, L49
- Shu, F. H. 1977, *ApJ*, 214, 488
- Shu, F. H., Najita, J. R., Shang, H., & Li, Z.-Y. 2000, *Protostars and Planets IV*, 789
- Smith, N., & Brooks, K. J., 2008, *Handbook of Star Forming Regions, Vol II*, B. Reipurth ed.
- Swift, J. J., & Welch, W. J. 2008, *ApJS*, 174, 202
- Tomisaka, K. 1998, *ApJ*, 502, L163
- Tóth, G. 2000, *Journal of Computational Physics*, 161, 605
- Truelove, J. K., Klein, R. I., McKee, C. F., Holliman, J. H., II, Howell, L. H., & Greenough, J. A. 1997, *ApJ*, 489, L179
- Vaillancourt, J. E., et al. 2008, *ApJ*, 679, L25
- Walawender, J., Bally, J., Francesco, J. D., Jørgensen, J., & Getman, K. 2008, *Handbook of Star Forming Regions, Volume I: The Northern Sky ASP Monograph Publications, Vol. 4*. Edited by Bo Reipurth, p.346
- Walmsley, M. 1995, *Revista Mexicana de Astronomia y Astrofisica Conference Series*, 1, 137
- Wang, P., & Abel, T., 2009, *ApJ*, in press
- Wolfire, M. G., & Cassinelli, J. P. 1987, *ApJ*, 319, 850
- Zhang, Q., Hunter, T. R., Brand, J., Sridharan, T. K., Cesaroni, R., Molinari, S., Wang, J., & Kramer, M. 2005, *ApJ*, 625, 864
- Zinnecker, H., & Yorke, H. W. 2007, *ARA&A*, 45, 481

Table 1. Model Characteristics

Model	Turbulence	Magnetic Field	Outflow	Stop Time
BASE	no	no	no	2.0
HD	yes	no	no	3.0
MHD	yes	yes	no	4.0
WIND	yes	yes	yes	5.525

Note. — The stop time of each simulation is given in units of the initial free-fall time at the clump center  $t_{\text{ff}} = 0.21$  Myr.

Table 2. Massive Objects at  $t = 3$

Name	Mass	$t_{\text{form}}$	#	Location	Notes
HD-A1	61.1	0.96	4	(0.66, 0.40, 0.48)	
HD-A2	22.6	1.36	1	(0.66, 0.40, 0.48)	
HD-A3	10.1	2.03	1	(0.68, 0.41, 0.48)	
HD-B1	21.3	1.11	1	(0.74, 0.48, 0.33)	
HD-B2	15.8	1.72	1	(0.74, 0.48, 0.33)	
HD-ALL	131		8		137 stars, $350M_{\odot}$ ; 37% massive
MHD-A1	12.3	1.05	1	(0.41, 0.34, 0.51)	
MHD-A2	46.7	1.35	2	(0.44, 0.38, 0.52)	
MHD-B1	14.6	2.30	1	(0.51, 0.65, 0.36)	
MHD-ALL	73.6		4		86 stars, $165 M_{\odot}$ ; 45% massive
WIND-ALL	0		0		72 stars, $69.7 M_{\odot}$ ; no massive stars

Note. — The units for the stellar mass, formation time, and stellar location are the solar mass, the initial free-fall time at the clump center, and the box size (2 pc). The 4th column denotes the number of stars in each generation. The number of all stars more massive than  $0.1 M_{\odot}$ , their total mass, and the fraction of the total stellar mass in massive objects are noted in the last column.

Table 3. Massive Objects at  $t = 4$

Name	Mass	$t_{\text{form}}$	#	Location	Notes
MHD-A1	15.0	1.05	1	(0.32, 0.45, 0.51)	
MHD-A2	110	1.35	2	(0.44, 0.40, 0.51)	
MHD-A3	12.5	3.13	1	(0.46, 0.41, 0.51)	
MHD-B1	45.8	2.30	1	(0.46, 0.65, 0.39)	
MHD-ALL	183		5		121 stars, 337 $M_{\odot}$ ; 54% massive
WIND-A1	16.9	1.16	1	(0.38, 0.42, 0.50)	
WIND-B1	10.5	2.29	1	(0.45, 0.68, 0.42)	
WIND-ALL	27.4		2		123 stars, 134 $M_{\odot}$ ; 20% massive

Note. — Units as in Table 2.

Table 4. Massive Objects at  $t = 5.5$

Name	Mass	$t_{\text{form}}$	#	Location	Notes
WIND-A1	46.4	1.16	1	(0.47, 0.36, 0.51)	
WIND-A2	11.8	1.34	1	(0.43, 0.33, 0.47)	
WIND-B1	16.7	2.29	1	(0.49, 0.67, 0.44)	
WIND-B2	12.0	2.31	1	(0.51, 0.67, 0.43)	
WIND-ALL	86.9		4		183 stars, 250 $M_{\odot}$ ; 35% massive

Note. — Units as in Table 2.

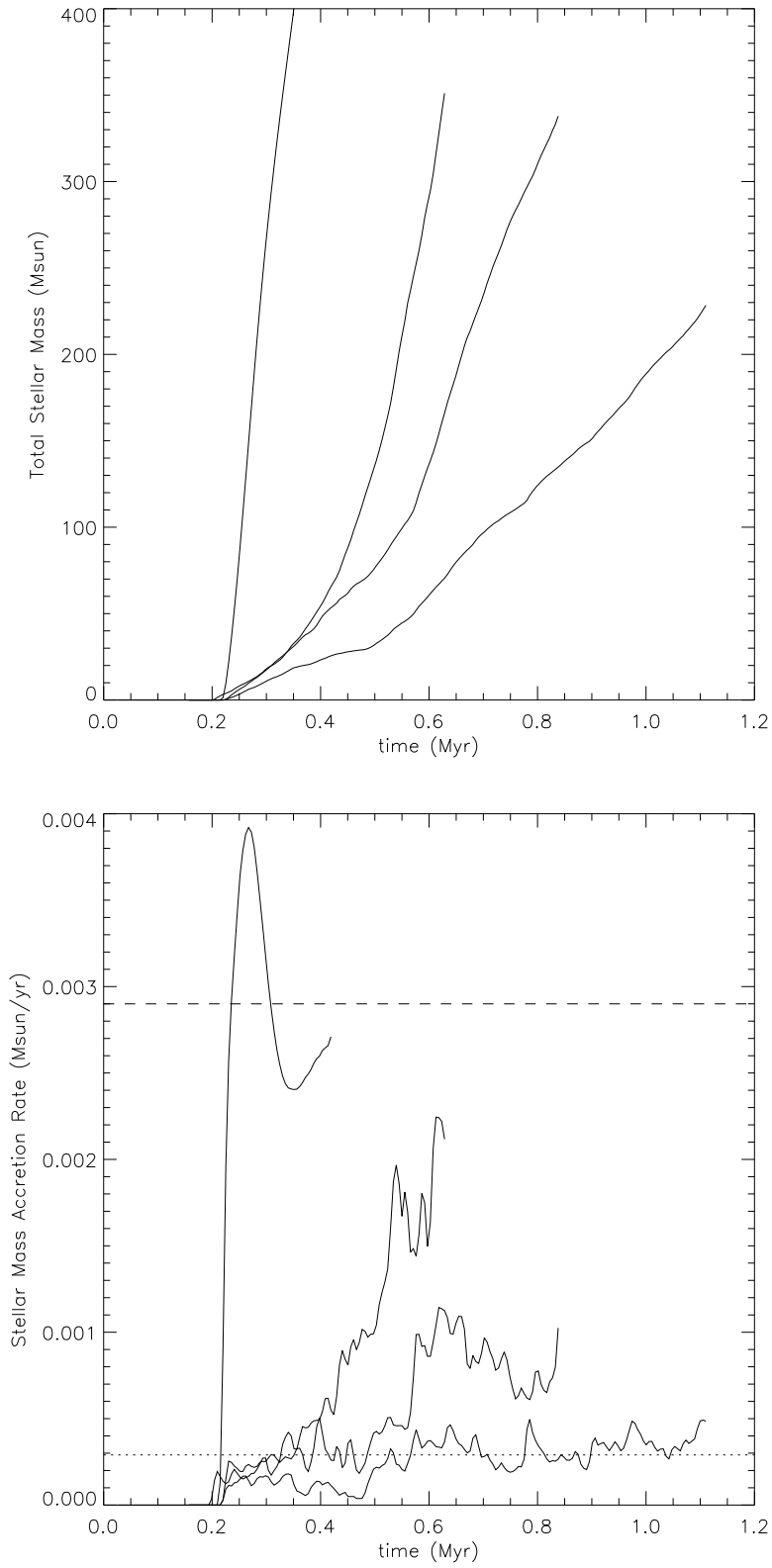


Fig. 1.— Evolution of the total stellar mass (top panel) and stellar mass accretion rate (bottom panel) for all 4 models. In each panel, the curves from upper-left to lower-right are for Model BASE, HD, MHD and WIND, respectively.

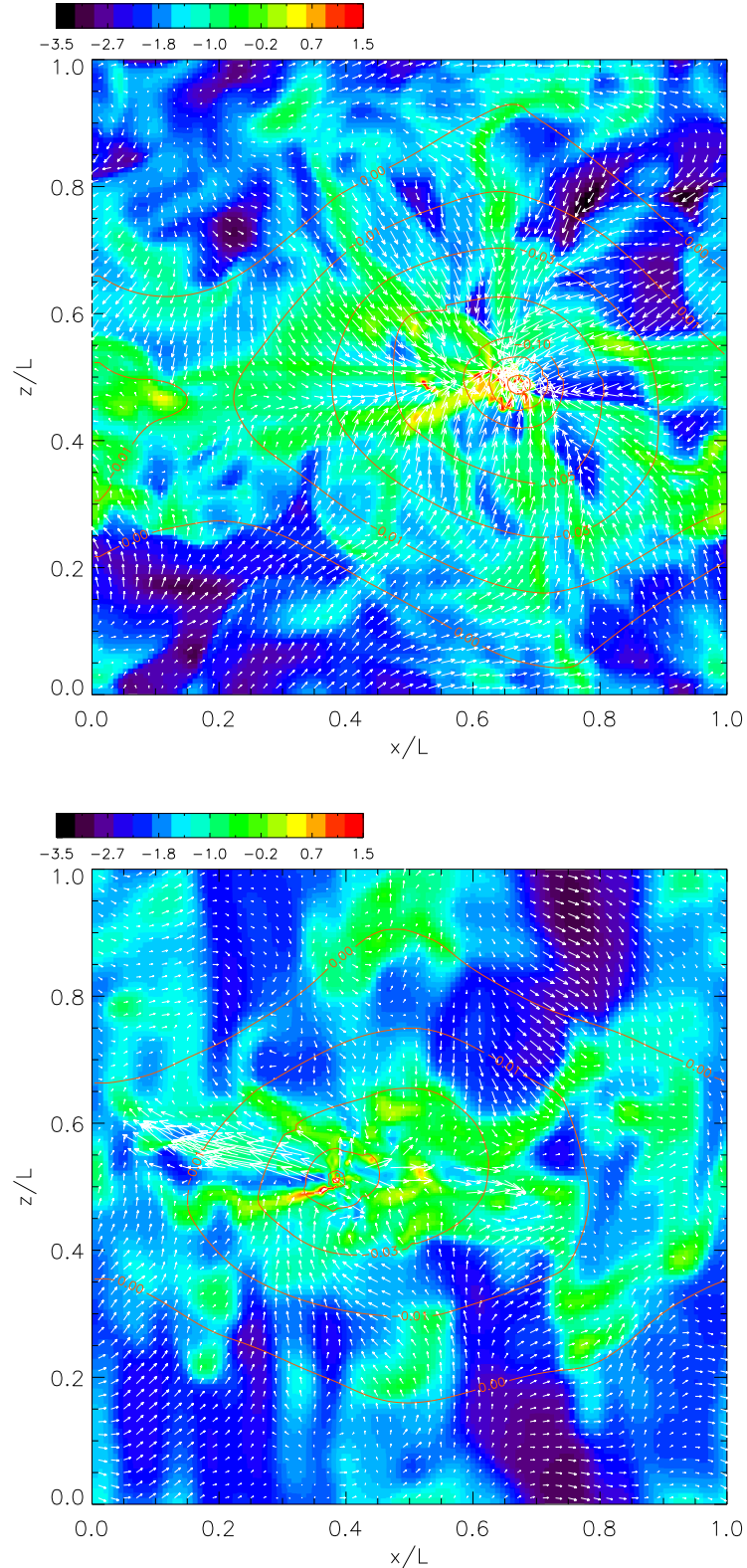


Fig. 2.— Density slice through the most massive object for the HD and WIND model at  $t=3$ . Overplotted are the velocity arrows (white) and contours of the gravitational potential. The colorbar is for the logarithm of the density in units of the initial central density of the clump, and length is scaled by the size of the simulation box  $L$ .

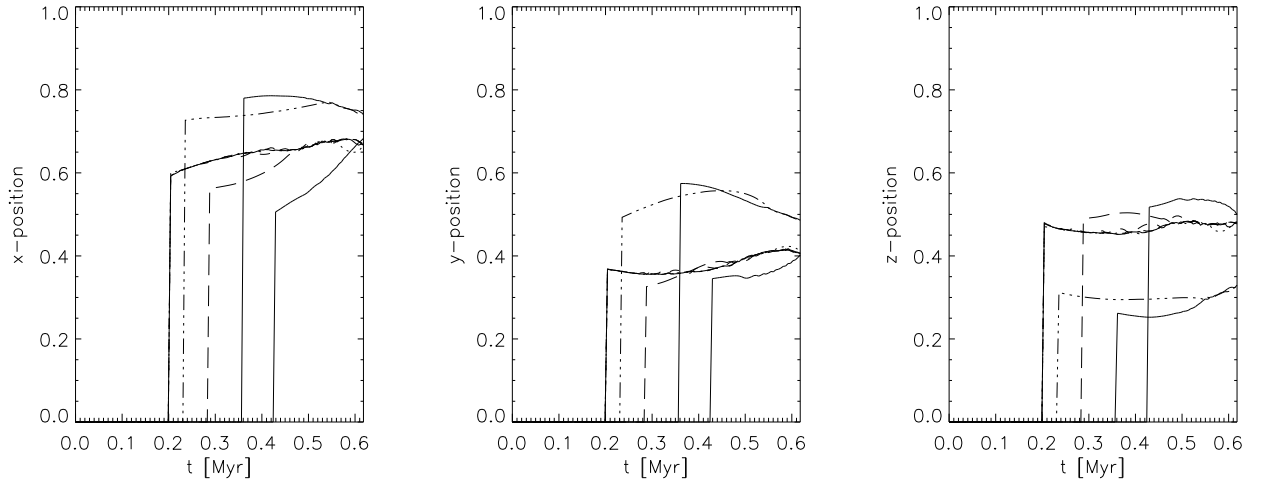


Fig. 3.— Evolution of the positions of the massive stars in the HD Model, showing the increase in the degree of clustering at later times.

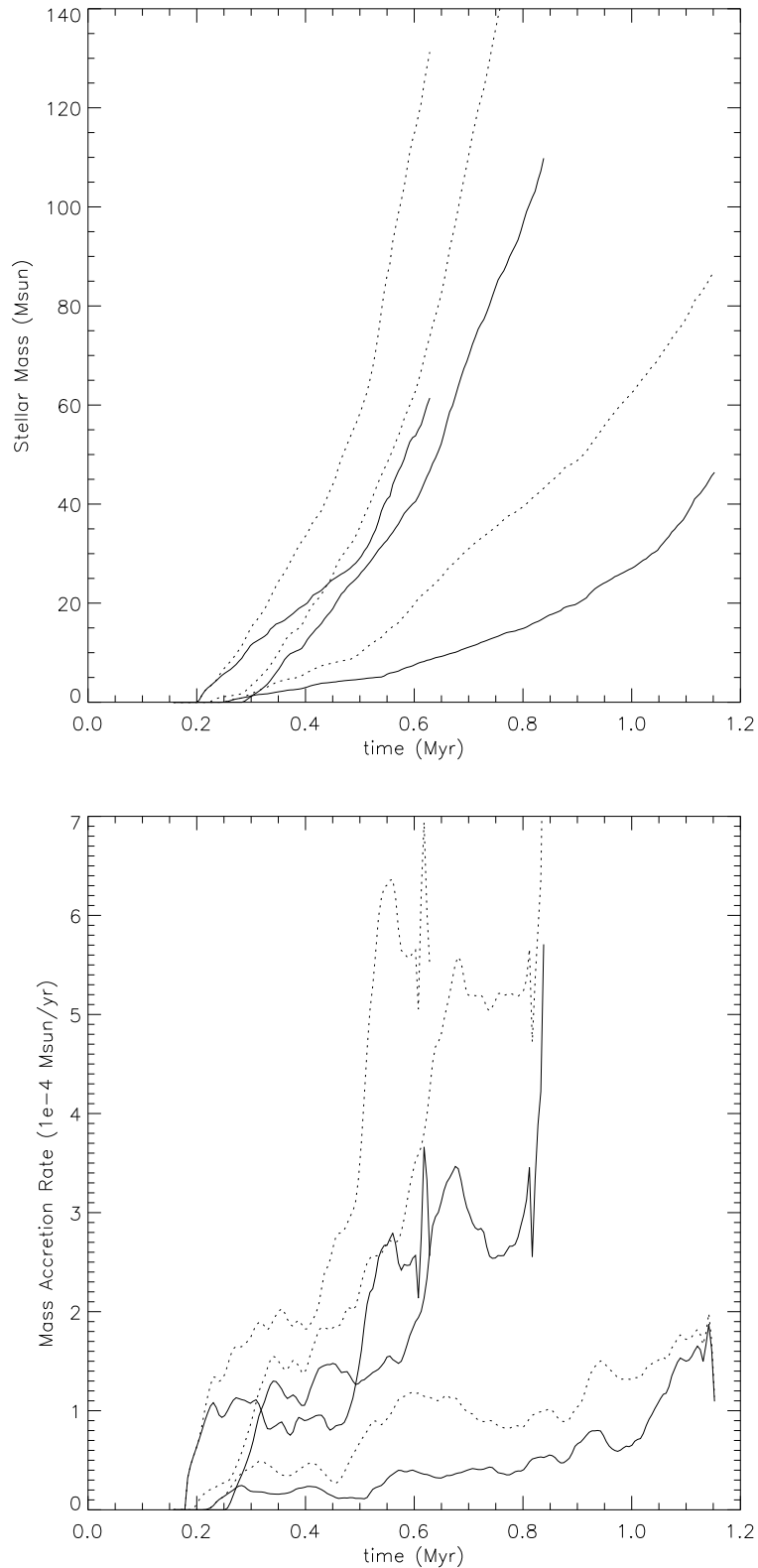


Fig. 4.— Evolution of the total mass (top panel) and mass accretion rate (bottom panel) of all massive stars (dotted lines) and those for the most massive object (solid lines). The curves from upper-left to lower-right are for Model HD, MHD and WIND, respectively.



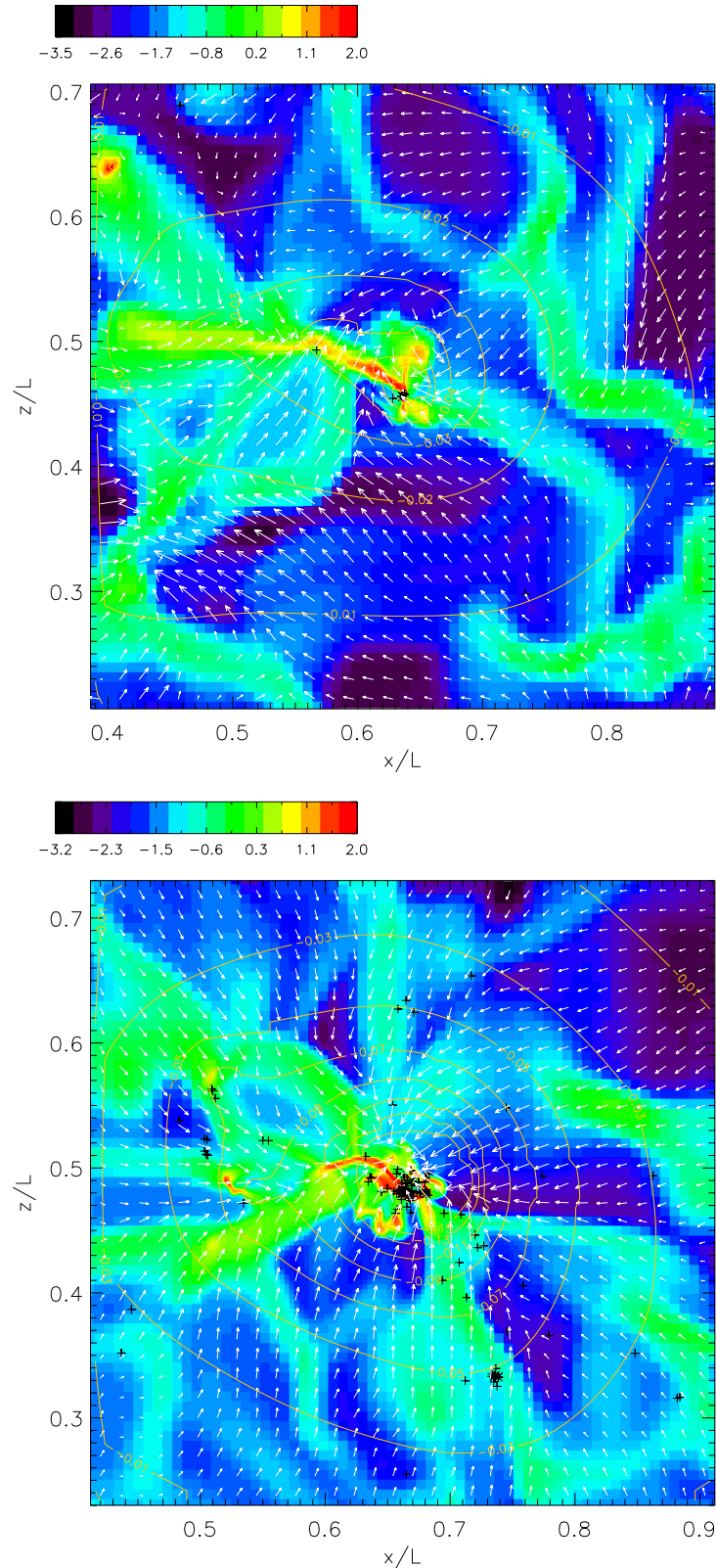


Fig. 5.— Slice of the density through the most massive object for the HD model, with the velocity vectors (white) and contours of the gravitational potential overplotted. The first panel shows the early phase of rapid mass accretion for the most massive object through a dense filament at  $t=1.5$ . The second shows the global collapse at  $t=3$ . Stars are denoted by

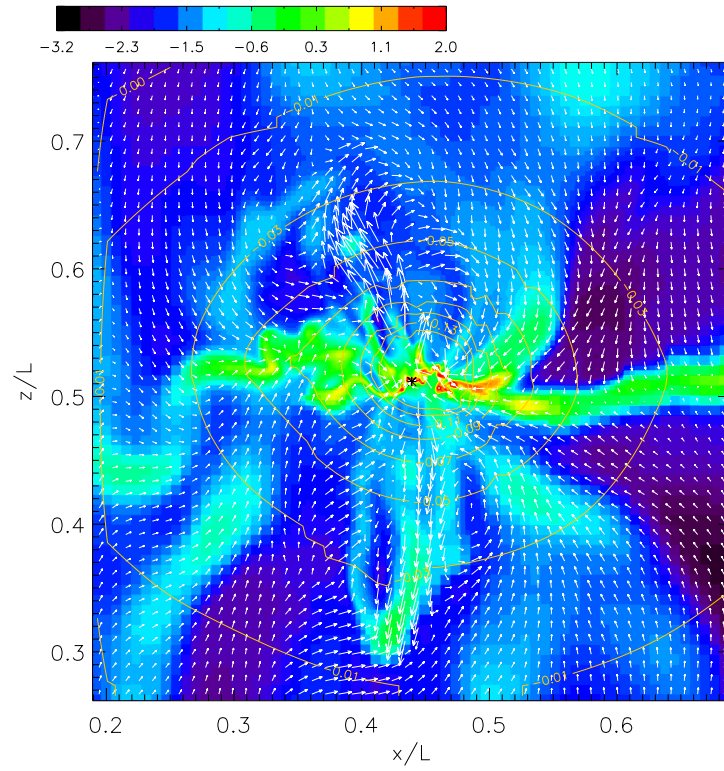


Fig. 6.— Slice of the density through the most massive object (denoted by an asterisk), showing a large magnetic bubble driven from near the central object at  $t=3.75$  in the MHD Model.

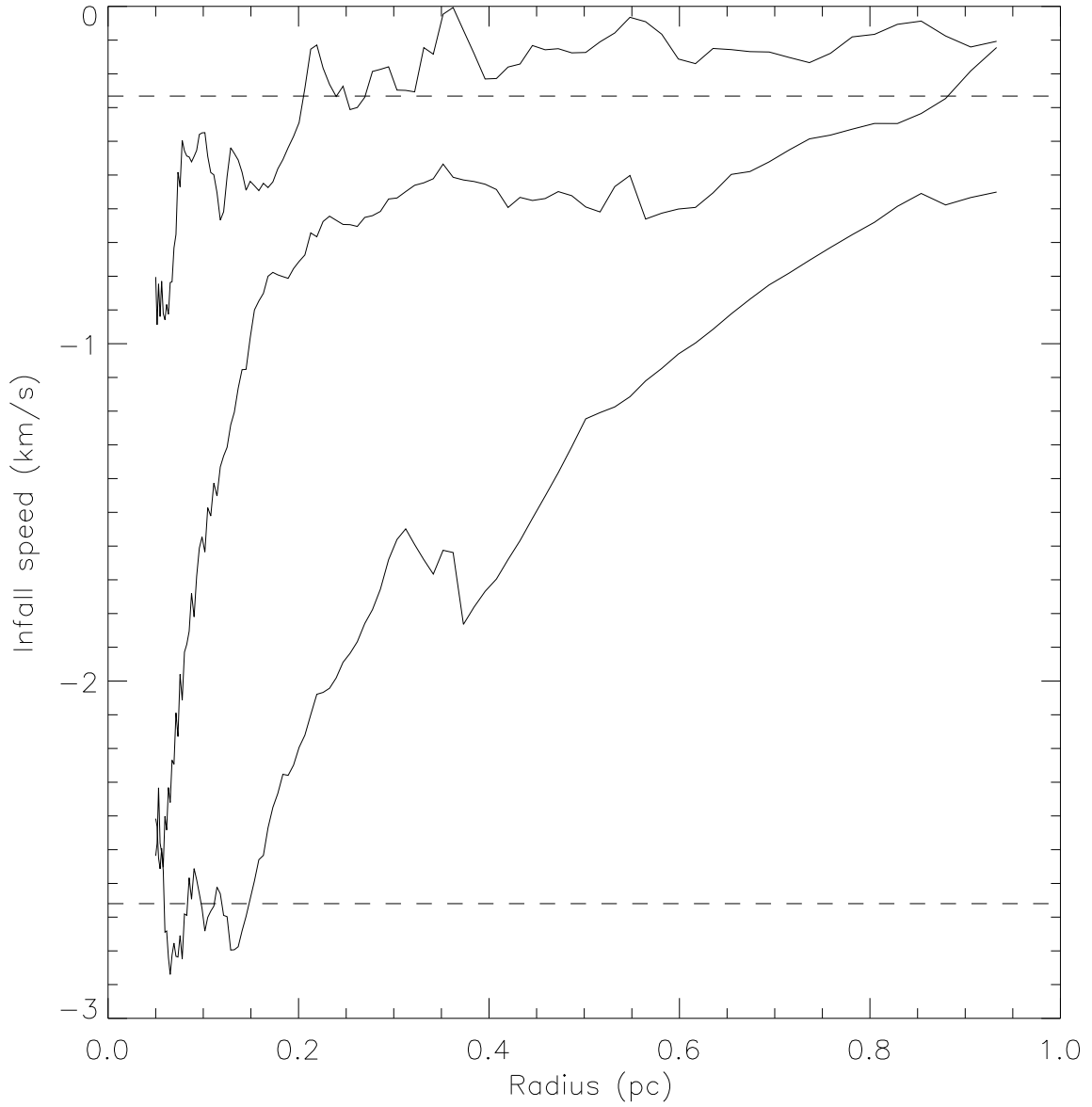


Fig. 7.— Radially averaged, mass-weighted, infall speed towards the most massive object for Model HD ( $t=3$ , bottom curve), MHD ( $t=4$ , middle curve) and WIND ( $t=5$ , top curve). The sound speed is plotted as dashed line for comparison.

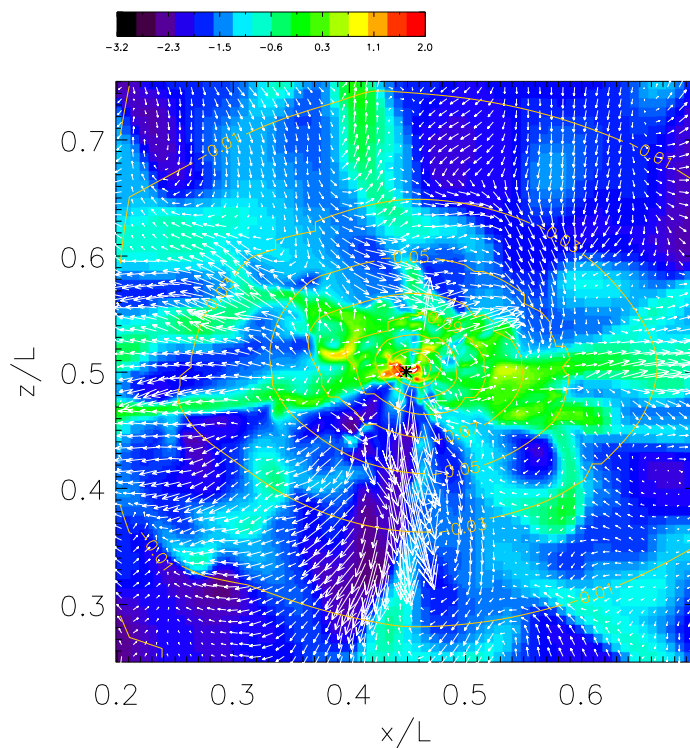


Fig. 8.— Slice of the density through the most massive object (denoted by an asterisk) in the WIND model at  $t = 5$ , showing a chaotic velocity field (denoted by white arrows), as opposed to the ordered global collapse in the HD case.

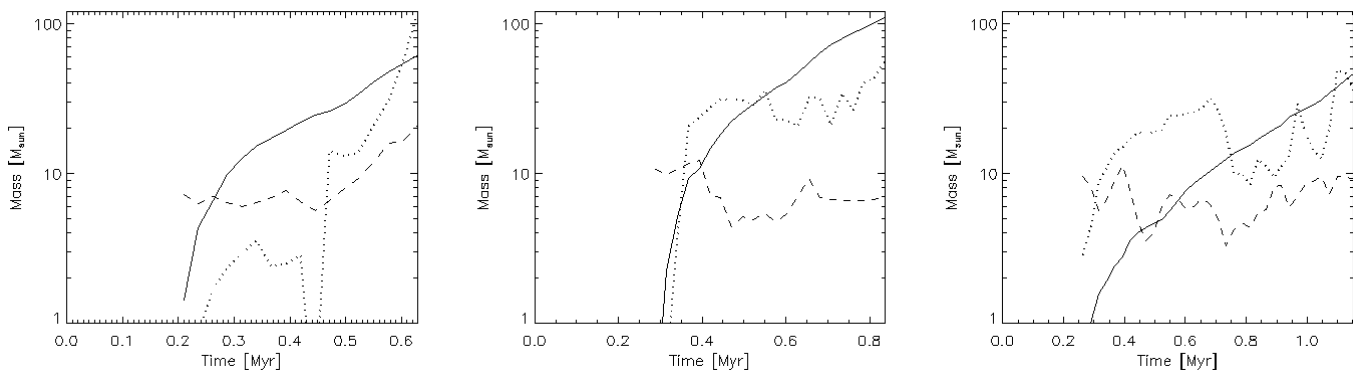


Fig. 9.— Time evolution of the mass of the most massive object (solid), and the masses of the gas (dashed) and other stars (dotted) within a “core” (defined as a sphere of 0.1 pc in diameter centered on the object) for the HD (left), MHD (middle) and WIND (right) models.